Author/s:
Patel, MK;Ryu, D;Western, AW;Suter, H;Young, IM

Title:
Which multispectral indices robustly measure canopy nitrogen across seasons: Lessons from an irrigated pasture crop

Date:
2021-03-01

Citation:
Patel, M. K., Ryu, D., Western, A. W., Suter, H. & Young, I. M. (2021). Which multispectral indices robustly measure canopy nitrogen across seasons: Lessons from an irrigated pasture crop. Computers and Electronics in Agriculture, 182, https://doi.org/10.1016/j.compag.2021.106000.

Persistent Link:
https://hdl.handle.net/11343/282490

Which Multispectral Indices Robustly Measure Canopy Nitrogen across Seasons: Lessons from an Irrigated Pasture Crop

Manish Kumar Patel[1a], Dongryeol Ryu[1], Andrew W Western[1], Helen Suter[2] and Iain M Young[3]

[1] *Department of Infrastructure Engineering, Melbourne School of Engineering, The University of Melbourne, Victoria 3010 Australia*

[2] *Faculty of Veterinary and Agricultural Sciences, School of Agriculture and Food, The University of Melbourne, Victoria 3010 Australia*

[3] *School of Life and Environmental Sciences, Faculty of Science, The University of Sydney, NSW 2006 Australia*

[a] *Corresponding author. E-mail address: manishp1@student.unimelb.edu.au (M K Patel).*

Abstract

In precision farming, accurate estimation of canopy nitrogen concentration (CNC) is valuable for effective crop growth monitoring and nitrogen (N) fertiliser management. To date, many canopy multispectral indices have been proposed as indicators for CNC; however, many of these indices have also shown sensitivity to biomass and their performance drops at high biomass levels. Dependence on growth stage, season, or other environmental conditions limits their efficacy as generalized CNC indices. The objectives of this study were to assess the robustness of popular CNC indices across a wide range of biomass levels and fertiliser application levels; and for two contrasting seasons – winter and summer. To achieve this, we analysed the efficacy of seven canopy nitrogen indices, including canopy chlorophyll content index (CCCI), together with eleven other commonly used spectral indices. We used canopy level solar-induced hyperspectral reflectance data acquired using a hand-held optical spectroradiometer across four growth stages in winter (May-June 2018) and four in summer (January-February 2019) from an experimental field of irrigated perennial ryegrass with variable N application in Victoria, Australia. The field contained 40 plots, each with one of

eight different N treatments. Almost all the indices exhibited similar correlation to CNC (%) when applied to individual stages (days) in both winter and summer; however, relationships between CNC and individual indices varied significantly between stages. We obtained similar results for canopy biomass. When the data across the entire range of growth stages and seasons were combined, the correlations between most canopy nitrogen indices and CNC became weak (R^2<0.25, 0.9%≤RMSE≤1.0%). PRI exhibited the highest correlation with CNC (R^2=0.58, RMSE=0.7%) for the combined data set. Even so, PRI's association with CNC and canopy biomass changed with the season. Most indices responded to both CNC and biomass simultaneously, and this confounds the estimation of CNC due to strong but growth stage-specific relationships between CNC and canopy biomass. This study shows that it is important to consider a wide range of conditions when evaluating multispectral CNC indices.

Keywords: Canopy nitrogen concentration; Vegetation index; N uptake; PRI; Canopy biomass

1. Introduction

The natural supply of nitrogen (N) from the soil is heavily supplemented by fertilisers in modern intensive cropping systems. Soil mineral N and its uptake by crops depends on soil characteristics, crop health and environmental variables that vary in space and time (Gupta et al., 1997; Mamo et al., 2003). Nevertheless, N fertilisers are generally applied homogeneously over a crop irrespective of spatial heterogeneity in crop N requirement and soil N status. Optimal spatial application of N fertiliser can reduce the economic and environmental costs of growing crops. Excess soil N induces emission of the greenhouse gas nitrous oxide (N_2O) (Mosier et al., 1998; Thompson et al., 2019) and, when leached, contaminates surface and groundwater systems (Wang and Li, 2019; Zhai et al., 2017).

The Nitrogen Nutrient Index (NNI), calculated as the ratio between actual Canopy Nitrogen Concentration (CNC) and critical CNC, has been shown to provide an accurate

measure of canopy N status (Lemaire et al., 2008; Plénet and Lemaire, 1999). The minimum CNC required to maintain the maximum growth is known as the critical CNC, which varies over the growth period. NNI values >1 indicate luxurious N consumption, while values <1 are linked to constrained N supply. The sensitivity of NNI to very small changes in crop N status and its usefulness for N status diagnosis, have made NNI a reliable and popular indicator for crop N status (Lemaire et al., 2008).

Unfortunately, field sampling and determining CNC in a laboratory from tissue analysis is time-consuming, destructive, and labour-intensive; limiting its routine application in crop management where high spatial and temporal resolution is required. In comparison, remote sensing can map CNC in a non-invasive and rapid manner frequently and at high spatial resolution, thereby aiding economic N fertiliser management. Canopy N monitoring at vegetative growth stages is important for site-specific fertilization (Cammarano et al., 2014; Fitzgerald et al., 2010) and continuous monitoring of canopy N across growth stages would yield high economic value (Hank et al., 2019).

Vegetation remote sensing is closely associated with plant chlorophyll, biomass, and water content, typically using contrasting response at different spectral reflectance bands to measure these variables (Curran, 1989; Fourty et al., 1996; Haboudane et al., 2004). Many authors have mentioned the close association between leaf optical reflectance and its chlorophyll content (Baret and Fourty, 1997; Basso et al., 2016; Clevers and Gitelson, 2013; Fourty et al., 1996; Hansen and Schjoerring, 2003; Sims and Gamon, 2002; Yoder and Pettigrew-Crosby, 1995). While there is no direct linkage between leaf reflectance attributes and N content in visible and near-infrared (NIR) (VNIR) bands, the correlation between leaf chlorophyll and N provides the missing link between spectral response and N in leaves (Baret and Fourty, 1997; Chen et al., 2010; Daughtry et al., 2000; Haboudane et al., 2002; Yoder and Pettigrew-Crosby, 1995).

Both multispectral (MS) and hyperspectral models have been used for CNC estimation and each has their own advantages. Here we concentrate on MS approaches. MS models use only a few spectral bands and are particularly advantageous in terms of cost, ease of sensor manufacture, tractability of data processing, ability to attain higher spatial resolution (for a given budget) and scaling up to airborne and satellite monitoring.

Several MS indices have been developed to estimate CNC at canopy level. Considering the relationship between chlorophyll and CNC, the response of chlorophyll in the visible and red-edge (a region of rapid change in reflectance from red to NIR) parts of the reflectance spectra provides one avenue to spectral indices for mapping CNC (Chen et al., 2010; Flowers et al., 2003; Gabriel et al., 2017; Li et al., 2014a; Zhang et al., 2006). A growing body of literature has examined red-edge based indices for mapping CNC (Chen et al., 2010; Clevers and Kooistra, 2011; Guo et al., 2017; Li et al., 2014a; Schlemmer et al., 2013; Sims and Gamon, 2002). Clevers and Gitelson (2013) presented red-edge band indices that explained up to 80% of the variance in N content in grass. Similarly, Fitzgerald et al. (2010) found a relationship between normalized difference red edge (NDRE) and CNC in winter wheat (R^2=0.55).

In addition to the changes in CNC, many extraneous factors such as canopy structural attributes (biomass, leaf area index (LAI) and leaf angle distribution (LAD)), view geometry, background reflectance and environmental properties also affect the responses of MS indices at canopy level (Cammarano et al., 2014; Haboudane et al., 2002; He et al., 2016; Van Leeuwen and Huete, 1996). Low-temperature plants tend to have higher N compared to plants grown at high temperature due to temperature directly affecting all physiological processes within plants. Thus, temperature controls the accumulation of N in leaves (Reich and Oleksyn, 2004). N application both induces changes in leaf CNC and modifies the canopy structural attributes (e.g. biomass) (Plénet and Lemaire, 1999). Consequently, changes in

canopy MS indices are driven by a combination of many factors, rather than leaf pigments alone (Asner, 1998; Chen et al., 2010; Daughtry et al., 2000; Haboudane et al., 2002; Stroppiana et al., 2009; Viña et al., 2011); with biomass being the most dominant factor (Stroppiana et al., 2009).

One important additional factor is LAI which can significantly affect the red-edge feature of a reflectance spectra when obtained at canopy level (Lamb et al., 2002). LAI has long been considered an important extraneous factor in designing spectral indices for pigment detection at the canopy scale. Daughtry et al. (2000) found that >98% of the variance in normalized difference spectral indices is associated with LAI. An example illustrating this issue is the Photochemical Reflectance Index (PRI), which is a narrow-band spectral index originally developed to track the xanthophyll cycle by Gamon et al. (1992). PRI can explain significant variability in maize and soybean chlorophyll content ($R^2 \geq 0.93$); however, it is also reported to be closely associated ($R^2 \geq 0.90$) with LAI (Gitelson et al., 2017). Barton and North (2001) also found that canopy PRI is not only related to the xanthophyll cycle but also influenced by LAI, LAD and background soil.

To fix one particular extraneous factor, background soil reflectance, which declines as LAI increases, Barnes et al. (2000) and Clarke et al. (2001) adopted an innovative approach in estimating cotton N concentration by using a two-dimensional index to compensate for changing canopy cover/soil influence on canopy N indices. The idea of this approach is that one index compensates for canopy cover to correct the CNC signal from a second index, and the result is referred to as the Canopy Chlorophyll Content Index (CCCI).

CCCI yielded a strong association ($R^2=0.95$) with CNC in cotton (Barnes et al., 2000). Encouraging results have also been obtained in mapping canopy N status using CCCI for a range of crops including cotton (Barnes et al., 2000; El-Shikha et al., 2008), wheat (Basso et al., 2016; Cammarano et al., 2014; Fitzgerald et al., 2010; Perry et al., 2012; Tilling et al.,

2007), broccoli (El-Shikha et al., 2007), and maize (Li et al., 2014a, 2014b). CCCI effectively eliminated the canopy cover induced variance and can be used as a N status indicator for canopy cover as low as 30% (El-Shikha et al., 2008).

Many N indices have shown joint sensitivity to CNC and biomass (Cammarano et al., 2014; Jay et al., 2017; Stroppiana et al., 2009) or have been found to be sensitive to biomass/LAI (Chen et al., 2010; Gitelson et al., 2017; Viña et al., 2011). Despite taking canopy cover into account, even CCCI has shown a close association with LAI and biomass (Cammarano et al., 2014; Li et al., 2014b). This raises an important question as to whether existing multispectral indices are more closely associated with CNC or biomass/LAI and implies that the performance of existing N indices as a predictor for CNC may rely on a consistent relationship between CNC and biomass. Such consistency may not exist.

A variety of factors are known to influence the relationship between CNC and biomass. For example, on one hand, increased N application tends to increase CNC and biomass for a given growth stage (e.g. Plénet and Lemaire (1999)), inducing a positive relationship with variable N application. On the other hand, considered over time, biomass typically has a negative relationship with CNC as the crop grows (Plénet and Lemaire, 1999). Together these two effects can lead to changing CNC-biomass relationship.

Taken together, the literature suggests that CNC indices should be assessed across a wide range of conditions. Assessment of the indices within a limited range of conditions may not reveal a) the confounding effects of CNC and biomass and b) the indices that are universally applicable across the wide range of CNC and growth conditions. In many studies, assessment of these indices was limited to one growth stage (e.g. Cammarano et al. (2014), Fitzgerald et al. (2010) and Tilling et al. (2007)). A small number of studies have reported that when assessed across the range of growth conditions, such as years, growth stages, and N application rates, the correlation of indices degraded rapidly due to changing relationship

between CNC and the relevant spectral indices (Feng et al., 2016; Li et al., 2014a, 2010; Stroppiana et al., 2009). The wide range of CNC-biomass relationships together with joint sensitivity of MS indices to both CNC and biomass makes selecting robust sensing algorithm challenging. Better understanding these interplays and how they impact different MS indices have the potential to improve the interpretation of algorithms, and that is the focus of this paper.

We examined the strength of relationship between each MS index and a) CNC and b) biomass for a range of growth stages, seasons and N application for irrigated pasture. In particular, we considered a wide range of MS indices that have been suggested for sensing CNC/chlorophyll. We did this for eight separate occasions and with combined data for winter, summer and the entire study. In addition, we characterized the changing relationship between CNC and biomass and evaluated changes in the relationships between CNC, biomass and MS indices.

2. Materials and Methods

2.1. Study area and datasets

The study site is located at Allansford, near Warrnambool (38°24'34.5"S, 142°38'13.0"E) in south-western Victoria, Australia. To investigate a wide range of growth and canopy N conditions, observations from perennial ryegrass (*Lolium perenne*) with different N treatments were analysed for several canopy conditions in each of two seasons, May-June (winter) 2018 and January-February (summer) 2019 (refer to Table 1 for measurement dates and pasture status (time since harvest)).

The field data collection was scheduled to cover four growth stages over a harvest-growth-harvest cycle (32 days in winter, 19 days in summer) for each season. The ryegrass was grown under the harvest-growth-harvest cycle in winter and summer seasons, and we

scheduled the first and last measurements to coincide with harvest events (first and the last harvest in a growth cycle). The remaining two measurements were performed sufficiently apart, depending on the biomass growth and logistics, the way through the growth cycle, resulting in four distinct measurements (Table 1). The last measurement dates, 18 June 2018 and 19 February 2019 were a day or two before the last harvest of the growth cycle.

Table 1. Field data collection dates, season, indicative growth stage and time since previous harvest. The growth stage number increases in the order of biomass development during the season.

Year & season	Measurement date	Growth stage name	Days of growth following harvest
2018 winter	17 May	CC-4	0, immediately prior to harvest
	25 May	CC-1	7
	04 June	CC-2	17
	18 June	CC-3	31
2019 summer	30 January	CC-4	1 day prior to harvest (31 January)
	07 February	CC-1	6
	15 February	CC-2	14
	19 February	CC-3	18

The abbreviation CC stands for canopy condition.

The experimental area was 29 m × 23 m and included 45 equal-sized 3 m × 3 m plots (Fig. 1), each of which received one of eight N treatments or zero N (control). One of three types of N fertiliser were used for the N treatment of each plot: urea (U, 46% N), urine (from dairy), and enhanced efficiency fertiliser (EEF, green Urea NV^{TM}). Five replicates of each application rate; 20, 40, 60, 80 kg/ha for U; 10, 20, 40 kg/ha for EEF, together with five control plots (no fertiliser, C) resulted in 40 plots with varying canopy N and biomass

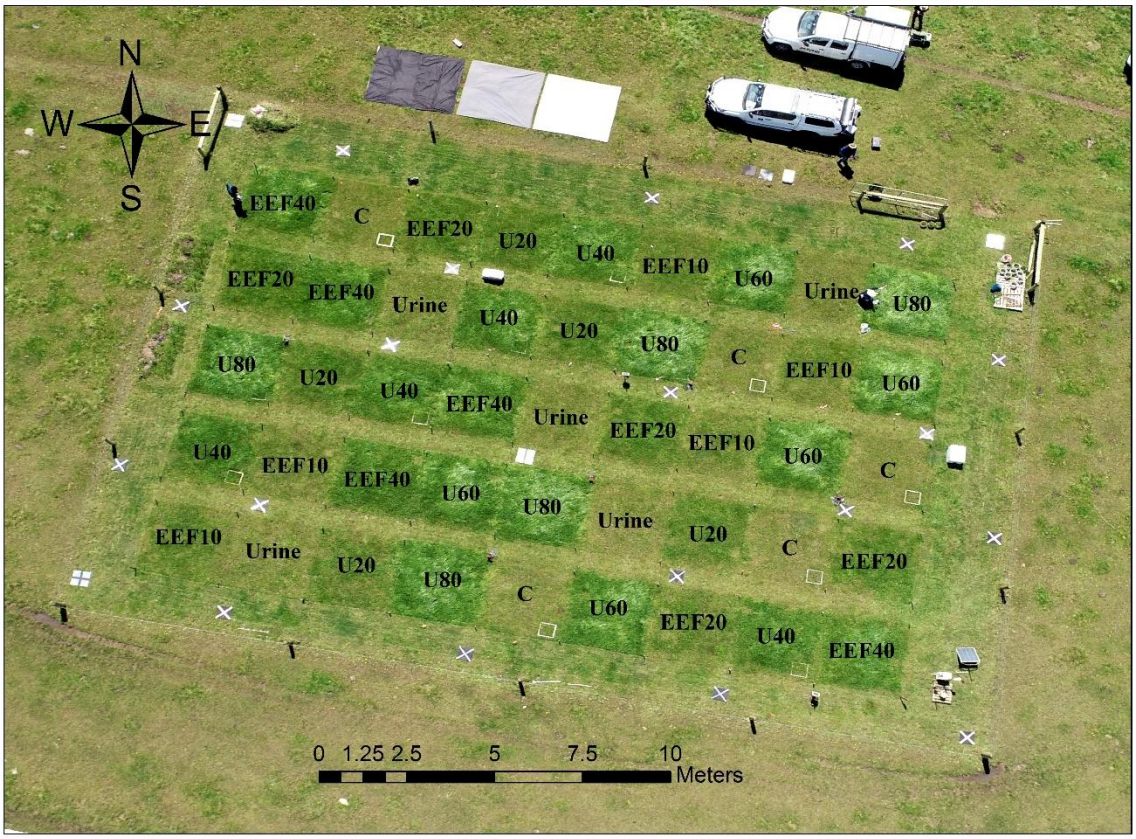

Fig. 1. Field site layout showing irrigated ryegrass plots with different N treatments indicated (19 February 2019). U, EEF and C represent urea, enhanced effective fertiliser and control treatments, respectively, and numbers indicate application rates. There is one randomly located replicate for each treatment in each of five east-west rows. (Double column image, colour)

conditions. The five urine treated plots were not considered in the analysis since the distribution of the urine within the treatment plots was found to be non-uniform. The variety of season, sampling time and N application ensures a wide range of growth conditions were incorporated to assess the robustness of the spectral indices.

Each 3 m × 3 m plot was divided into 0.3 m × 0.3 m sampling sections. A randomly selected sampling section was then measured with an ASD spectroradiometer, followed by destructive sampling and laboratory analysis of the ryegrass canopy for CNC and canopy biomass determination; without overlap of sampling sections between successive sampling

193 dates.

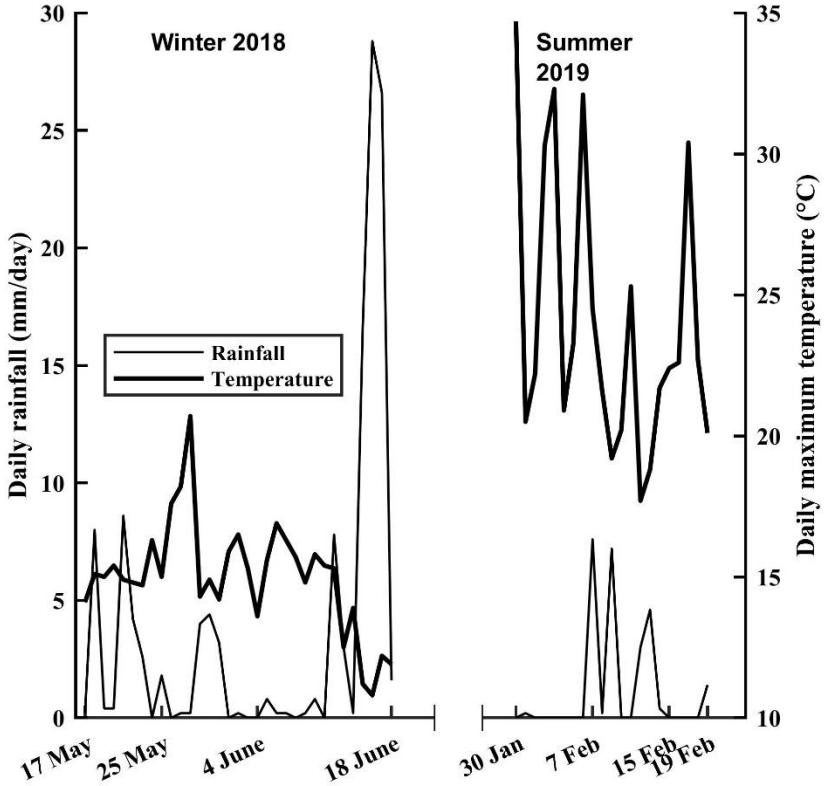

Fig. 2. Daily maximum temperature and rainfall during the winter 2018 and summer 2019 experimental periods. Data source is the Australian Bureau of Meteorology, station 90186 Warrnambool airport NDB station. (Single column image)

194 Fig. 2 shows the weather conditions (daily rainfall depth and maximum temperature)
195 during the data collection period in winter 2018 and summer 2019. The area has oceanic
196 weather with a temperate climate. Overall average temperatures of around 15°C and 24°C
197 were observed in winter 2018 and summer 2019 respectively during the data collection
198 period. Sufficient soil moisture was maintained to ensure it was not a limiting factor by using
199 a centre pivot irrigation system.

200 *2.2. Spectroradiometer data collection*

201 The canopy-level solar-induced reflectance data were collected over a 0.3 m × 0.3 m

sampling section within each plot. The canopy reflectance was measured using an Analytical Spectral Devices (ASD) HandHeld-2 field spectroradiometer (Analytical Spectral Devices, Inc., Boulder, CO, USA) between 12:00 and 14:35 local time. The device was warmed up for approximately 20 minutes prior to sampling. To convert the spectral radiance to reflectance and to compensate for changes in solar illumination, spectra were frequently captured from a 99% Spectralon ($BaSO_4$) panel (Labsphere, Inc., North Sutton, NH, USA) during the sampling. Spectra collection was mostly under the partly cloudy to cloudy conditions due to the coastal location.

The ASD HandHeld-2 spectroradiometer has a spectral measurement range of 325-1075 nm, with a spectral resolution of 3.5 nm and a spectral sampling interval of 1.6 nm. An inbuilt interpolation algorithm provided 1-nm interval spectral reflectance in the final output spectra. Therefore, each measured spectrum consisted of a total of 751 reflectance points with 1-nm intervals ranging from 325-1075 nm.

To obtain a representative canopy level reflectance value for the ground truth sampling area and to reduce measurement variability, 25-30 repeat scans were obtained at approximate heights of 33 cm and 67 cm above the canopy in the nadir position. With a 25º field of view, this configuration produced sampling footprints of approximately 0.15 m and 0.30 m in diameter, respectively. These were then averaged together.

2.3. Laboratory processing of ryegrass samples

Immediately after canopy reflectance measurement, the grazeable biomass was harvested. Grazeable biomass comprised most of the above-ground biomass within the 0.3 m × 0.3 m sampling sections was harvested. Sampling was done by cutting at approximate grazing height (~5-7 cm above the soil level). The resulting samples contained the whole canopy and left only stems for the regrowth. Ryegrass samples were preserved in a cold box containing ice for transport to the University of Melbourne laboratory (4-5 hours after

sampling). The fresh biomass was then weighed, and samples were dried at a constant temperature of 70ºC until they reached a stable dry weight (72-96 hours). Then the dry biomass as a measure of canopy biomass, was determined.

Following drying, samples were ground and processed for N analysis. The Dumas Combustion – LECO Trumac method (Matejovic, 1995) was used to determine the CNC (percent of dry weight) from the ground plant samples using a furnace temperature of 1350ºC. The N uptake (kg-N/ha) was calculated by multiplying the CNC (g-N/g-canopy biomass) with canopy biomass (kg/ha).

2.4. Multispectral reflectance indices

Eighteen remote sensing indices commonly used for N status and/or chlorophyll estimation at the canopy scale were selected to evaluate their robustness across the changing growth stages and different seasons. Table 2 lists the spectral indices used in this study and the reflectance bands used to calculate them. Based on the literature survey, NDRE, mSR, DCNI, AIVI, WRNI and planar domain indices (CCCI and CCCI-mSR) are grouped as canopy nitrogen indices. Most of the band-difference-ratio based indices in Table 2 were calculated using 10-nm bandwidths centred at the indicated wavelength. An exception was PRI, which was calculated using a 3-nm bandwidth (Trotter et al., 2002).

Planar domain indices designed to compensate for the canopy-cover changes in estimating the canopy N status (Barnes et al., 2000; Clarke et al., 2001) were also used. The variability in canopy cover mostly comes from the growth dependent LAI/leaf development of the crop. In a planar domain index, one of the dimensions uses an index sensitive to canopy cover and the other uses an N sensitive index. NDVI is a routine choice for the canopy cover index in the CCCI literature (Barnes et al., 2000; Cammarano et al., 2014; Fitzgerald et al., 2010) and we have followed that practice here. Two planar domain indices were evaluated – CCCI and CCCI-mSR. These used NDRE and mSR as indices sensitive to canopy N,

Table 2. List of spectral indices used for CNC and/or chlorophyll status estimation in this study.

Index	Formula	Reference
One dimensional index		
NDVI (Normalized Difference Vegetation Index)	NDVI = (R800 - R670) / (R800 + R670)	Rouse Jr et al. (1973)
SAVI (Soil Adjusted Vegetation Index)	SAVI = (1 + L) × (R800 - R670) / (R800 + R670 + L); L=0.5	Huete (1988)
PRI (Photochemical Reflectance Index)	PRI = (R531 - R570) / (R531 + R570)	Gamon et al. (1992)
TCARI (Transformed Chlorophyll Absorption in Reflectance Index)	TCARI = 3 × [(R700 - R670) - 0.2 × (R700 - R550) × (R700 / R670)]	Kim et al. (1994)
NPCI (Normalized Pigment Chlorophyll Ratio Index)	NPCI = (R680 - R430) / (R680 + R430)	Peñuelas et al. (1994)
SIPI (Structural Insensitive Pigment Index)	SIPI = (R800 - R445) / (R800 - R680)	Penuelas et al. (1995)
OSAVI (Optimised Soil-Adjusted Vegetation Index)	OSAVI = (1 + 0.16) × (R800 - R670) / (R800 + R670 + 0.16)	Rondeaux et al. (1996)
NDRE (Normalized Difference Red Edge)	NDRE = (R790 - R720) / (R790 + R720)	Barnes et al. (2000)
CCII (Canopy Chlorophyll Inversion Index)	CCII = TCARI / OSAVI	Haboudane et al. (2002)
EVI (Enhanced Vegetation Index)	EVI = 2.5 × (R860 - R645) / (1 + R860 + 6 × R645 - 7.5 × R470)	Huete et al. (2002)
mND705 (Modified Red-Edge Normalized Difference Vegetation Index)	(mND705) = (R750 - R705) / (R750 + R705 – 2 × R445)	Sims and Gamon (2002)
mSR (Modified Simple Ratio)	mSR = (R750 - R445) / (R705 - R445)	Sims and Gamon (2002)
MTCI (MERIS Terrestrial Chlorophyll Index)	MTCI = (R750 - R710) / (R710 - R680)	Dash and Curran (2004)
DCNI (Double-peak Canopy Nitrogen Index)	DCNI = (R720 - R700) / (R700 - R670) / (R720 - R670 + 0.03)	Chen et al. (2010)
AIVI (Angular Insensitivity Vegetation Index)	AIVI = [R445 × (R720 + R735) - R573 × (R720 - R735)] / [R720 × (R573 + R445)]	He et al. (2016)
WRNI (Water Resistance Nitrogen Index)	WRNI = NDRE / fWBI*	Feng et al. (2016)
Planar domain index		

CCCI (Canopy Chlorophyll Content Index)	CCCI = (NDRE - $NDRE_{min}$) / ($NDRE_{max}$ - $NDRE_{min}$)	Barnes et al. (2000)
CCCI-mSR	CCCI-mSR = (mSR - mSR_{min}) / (mSR_{max} - mSR_{min})	Rodriguez et al. (2006)

Note. RXXX represents the reflectance value at centre wavelength XXX nm. fWBI* = R900 / min (R930-980) (Strachan et al., 2002).

252 respectively, and NDVI to represent canopy cover (Fitzgerald et al., 2010, 2006; Rodriguez et
253 al., 2006). Fig. 3 illustrates the concept. Lower and upper bound lines of NDRE (or mSR) vs.
254 canopy cover (NDVI) are determined, and the index is then calculated by scaling the

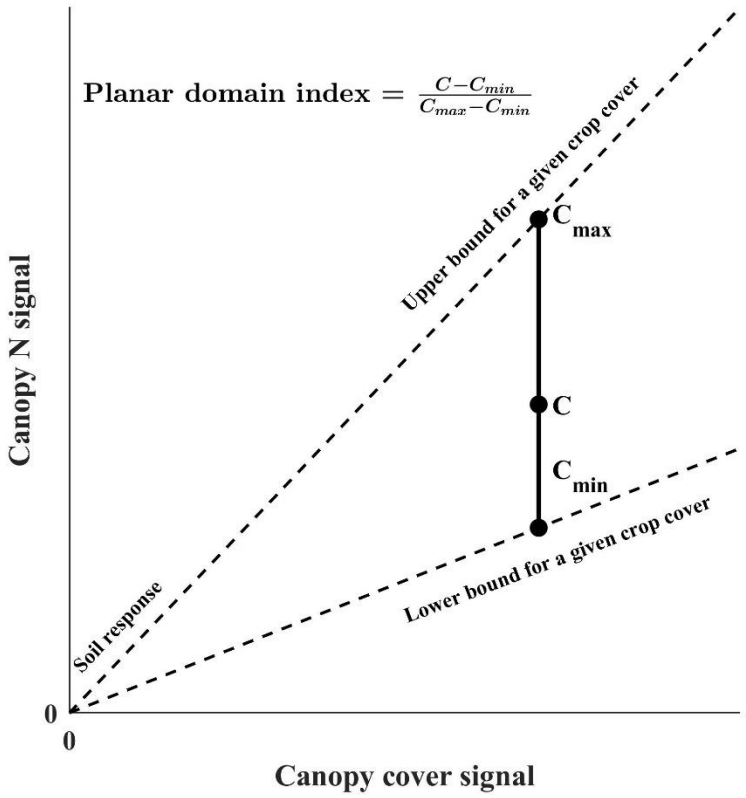

Fig. 3. Schematic illustration of the planar domain index calculation. (Single column image)

255 measured NDRE (or mSR) between the upper and lower bounds, which are determined from
256 the measured NDVI using the bounding lines. The upper and lower bound relationships

between NDRE (or mSR) and NDVI, were defined using 1.1 × maximum and 0.9 × minimum of ratio of NDRE (or mSR) to NDVI the dataset for the particular growth stage.

The intersection of the upper and lower bounds at the origin corresponds to the hypothetical bare soil response. The planar domain indices have values between 0 and 1 for all possible cases of canopy cover; however, values other than this range are also possible when data lies outside the lower or upper bounds.

2.5. Statistical analyses

The relationship between remote sensing indices and crop variable (CNC and canopy biomass) were quantified using standard regression analysis. The coefficient of determination (R^2), root mean square error (RMSE) and normalized RMSE (NRMSE) were used as performance metrics for assessing the degree of association in the relationships and their precision. It should be noted that here these are measures of fit, not the predictive skill, as no independent validation has been undertaken, given the aims of the study. The relationship between each spectral index and crop variable was established using popular two-parameter univariate regression models: linear (L), logarithmic-linear (Ll), linear-logarithmic (lL), exponential (E) and power (P) models (Table 3). Quadratic fit, a three-parameter model, was also tested but produced minor changes and did not change the overall conclusion. Relationships were developed for individual groups based on growth stage (CC-1, 2, 3 and 4) and season (winter and summer), and to the entire data set separately. PRI was only fitted with L, Ll and E models due to the presence of negative values. The relationship chosen and the statistics quoted in each case were based on the best performance according to RMSE. RMSE and NRMSE were calculated using:

$$RMSE = \sqrt{\frac{1}{N-p} \times \sum_{k=1}^{N} \left(Y^{k}_{predicted} - Y^{k}\right)^{2}}, \quad (1)$$

280 $$NRMSE = \frac{RMSE}{\bar{Y}} \times 100, \quad (2)$$

281 where Y, $\bar{Y}$, $Y_{predicted}$, N *and* p are the observed crop variable (CNC and canopy biomass),
282 arithmetic mean of Y, predicted crop variable, number of observations and number of
283 parameters in the regression equation (e.g. p=2 for two parameter models), respectively. The
284 standard Spearman rank correlation coefficient (r) was used to quantify the strength and
285 direction of monotonic relationship between CNC and canopy biomass.

Table 3. Model functional forms. a is a regression coefficient and b is an intercept term. X is a remote sensing index and Y is a crop variable (i.e. CNC or canopy biomass). The letters in bracket next to each model name give the abbreviation for that model.

Model	Functional formula
Linear (L)	$Y = a \cdot X + b$
Exponential (E)	$Y = a \cdot e^{X} + b$
Logarithmic-linear (Ll)	$\ln Y = a \cdot X + b$
Linear-logarithmic (lL)	$Y = a \cdot \ln X + b$
Power (P)	$\ln Y = a \cdot \ln X + b$

286 **3. Results**

287 *3.1. Variability of canopy N and canopy biomass*

288 CNC, canopy biomass and N uptake derived from the ground biomass samples varied
289 markedly with growth stage and season (Table 4). Fig. 4 shows the high variability in CNC
290 and canopy biomass, which was due to the combination of variable N fertiliser application
291 and different growth stages. While overall CNC shows a declining trend with canopy biomass
292 across growth stages in both seasons, CNC increases with canopy biomass at each growth
293 stage (Fig 4a,b). Fig 4c,d shows the behaviour of some distinct N treatment groups (U80,

U40, U20 and C) across the growth stages. In general, higher N treatment groups, for example, U80 had high CNC and canopy biomass compared to lower N treatment groups (such as C) at a given growth stage, but CNC diluted as biomass increased for any given N treatment. Due to the combination of these opposing trends, CNC vs. canopy biomass from our experimental site features significantly wider scatter than conventional 'dilution curves' constructed from uniformly fertilised fields.

Table 4. Canopy biomass, CNC and N uptake of ryegrass at four growth stages of winter and summer.

		Winter 2018				Summer 2019			
		CC-1	CC-2	CC-3	CC-4	CC-1	CC-2	CC-3	CC-4
Canopy biomass (kg/ha)[a]	mean	370	600	990	1540	560	880	1240	1450
	std	120	180	320	470	180	510	590	590
	CV	0.32	0.30	0.32	0.31	0.32	0.58	0.48	0.41
CNC (%)	mean	4.1	4.5	4.1	3.7	3.1	2.7	2.4	2.0
	std	0.5	0.5	0.5	0.5	0.8	0.5	0.5	0.4
	CV	0.12	0.11	0.12	0.14	0.26	0.19	0.21	0.20
N uptake (kg-N/ha)[a]	mean	15	28	42	58	18	27	33	30
	std	6	10	16	19	08	19	22	17
	CV	0.40	0.36	0.38	0.33	0.44	0.70	0.67	0.57

Note: std - standard deviation; CV- coefficient of variation (std/mean); [a] denotes area measurements are based on ground area. Sample size (*n*) is 40 for values in the table.

CNC varied over two quite different ranges in winter and summer (2.8% - 5.4% in winter, and 1.3% - 4.3% in summer). On average, CNC values were 58% higher in winter than summer. The observed decrease in summer season CNC is attributed to the influence of temperature on physiological processes within the plants leading to a decrease in leaf N in warm weather (Reich and Oleksyn, 2004). Response to different N treatments are more

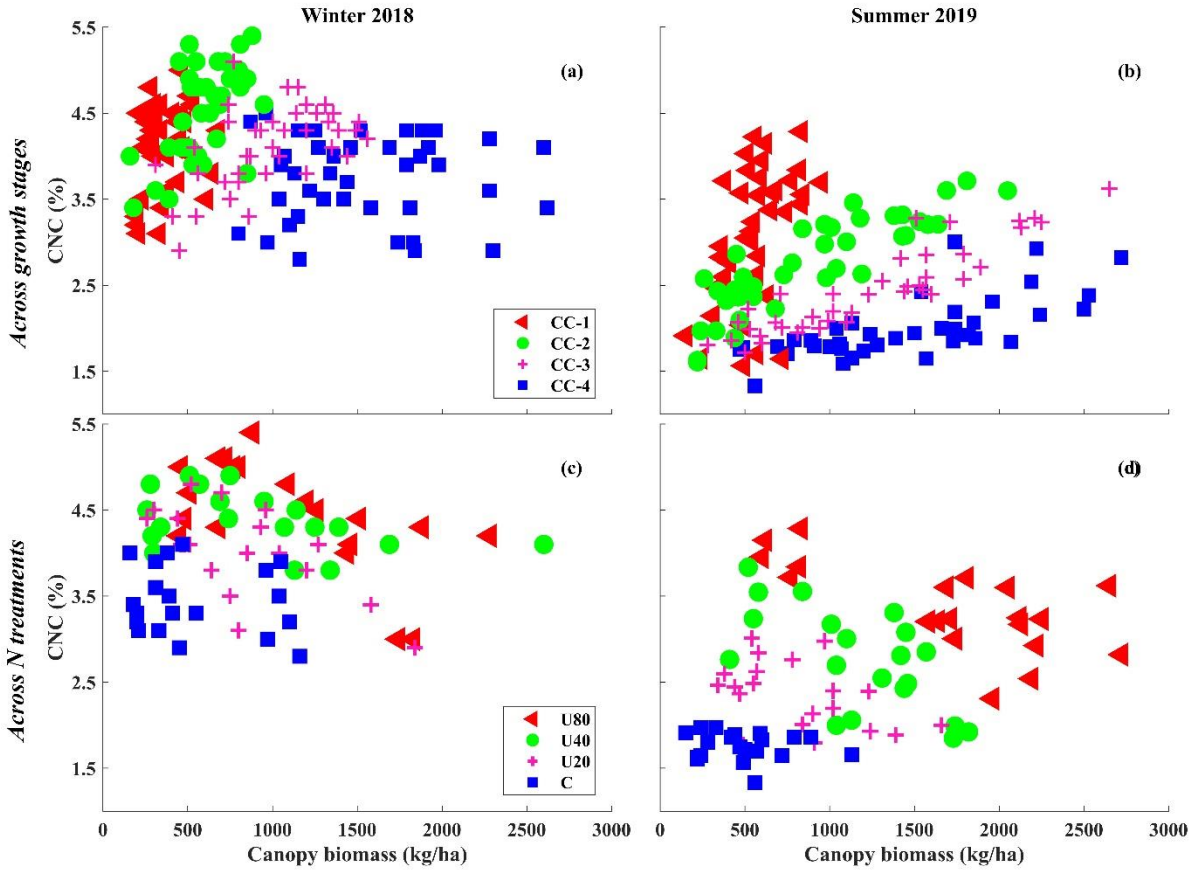

Fig. 4. Scatter plots of CNC (%) and canopy biomass (kg/ha). (a) and (b) show summer and winter results respectively, combined across all N application rates for each sampling occasion. (c) and (d) show summer and winter results respectively for selected N treatment groups; U80, U40, U20 and C. (Double column image, colour)

distinct in summer than in winter (Fig. 4c,d). CNC reduced as the sward grew in both seasons, with mean CNC declining from 4.1% to 3.7% (approximately 10%) in winter and3.1% to 2.0% (approximately 36%) in summer for CC-1 to CC-4, respectively. The variability, as measured by CV, remained relatively consistent within each season, compared with the difference in CV between seasons (Table 4). The overall variance in CNC with respect to both treatments and growth stages was almost double in summer compared with winter.

More rapid biomass growth occurred in summer than winter with average canopy

biomass being 17% higher and the harvest-growth-harvest cycle being 42% shorter in summer than winter. Despite this difference, the range of biomass in both summer and winter remained comparable (Fig. 4). Variation (standard deviation) in canopy biomass was also higher in summer than winter after CC-1, increased with biomass. Biomass variability, as measured by CV, was higher for summer growth stages (except CC-1), than winter, and peaked for the middle growth stages in summer while remaining flat in winter (Table 4). On average, summer growth stages exhibited higher variance in both CNC and canopy biomass compared to winter (Table 4). In contrast to CNC, winter canopy biomass exhibited slightly (around 7%) higher variance than summer.

In addition to CNC, N uptake is commonly used as a measure of canopy N content when remote sensing is used to estimate crop N. Variance of N uptake followed a similar pattern to canopy biomass, with summer growth stages exhibiting a higher CV (Table 4). Generally, mean N uptake increased with canopy biomass. The exception was CC-4 in summer when N uptake decline from its value at CC-3 due to the declining CNC (Table 4). N uptake demonstrated a very high correlation with canopy biomass ($0.86<r<0.99$) on all sampling occasions (Fig. 5), whereas the correlation between CNC and canopy biomass changed with growth stage ($0.01<r<0.90$). These results suggest that N uptake is largely determined by the canopy biomass with little information on CNC. Therefore, CNC will be used in the subsequent sections to analyse canopy N vs. canopy biomass relationship and to evaluate the association of the chosen MS indices. Both the correlation ($0.01<r<0.90$) and the relationship between CNC and canopy biomass varied across a wide range depending on individual growth stages (Fig. 5). The correlation increased from CC-1, peaked at CC-2 ($r=0.49$) in winter and CC-3 ($r=0.90$) in summer, and then declined. A risk in analysing performance is that this high correlation could confound the distinct spectral attributes of CNC at some growth stages.

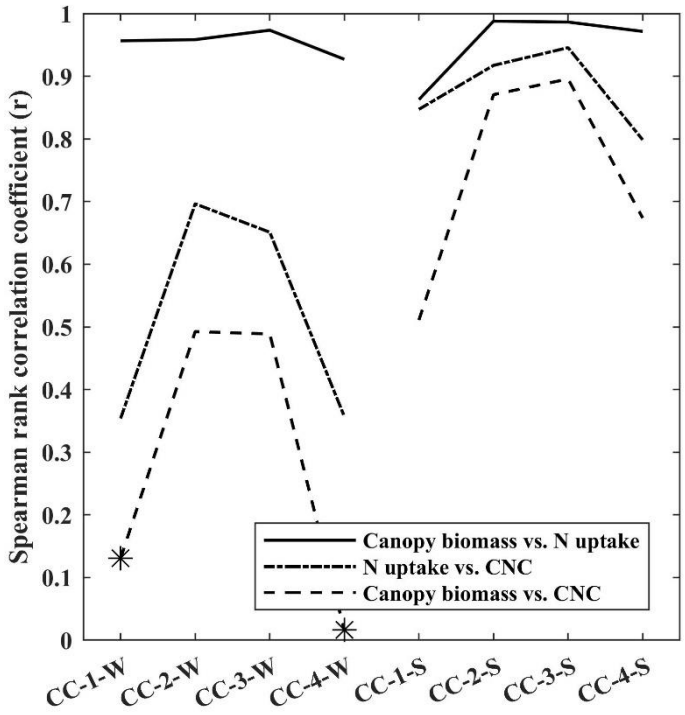

Fig. 5. Spearman rank correlation (r) between CNC (%), canopy biomass (kg/ha) and N uptake (g-N/m^2) over the growth stages in winter 2018 and summer 2019 (n=40). W and S indicate winter and summer seasons, respectively. * indicates correlation not statistically significant (p>0.05). (Single column image)

3.2. Relationship between spectral indices and crop variables (CNC and canopy biomass) at individual growth stages

The most important criteria for the selection of a remote sensing index are a high correlation with the target variable (CNC in this case) and low sensitivity to the other confounding factors (Daughtry et al., 2000). Fig. 6 and Fig. 7 show R^2 and NRMSE for the CNC and canopy biomass estimated by 18 remote sensing indices at each growth stage (see corresponding tables, Table S1 and S2 in the supplementary material). While there was contrasting performance between stages, most of the indices exhibited similar performance at individual growth stages, except for TCARI, CCII and DCNI. The best index varied between

346 stages, but the difference between indices in explaining either CNC or canopy biomass
347 variation was small within the growth stage. For instance, PRI (R^2=0.46, RMSE=0.4%) was
348 best for CC-2 during winter while OSAVI (R^2=0.84, RMSE=0.2%) was best for CC-2

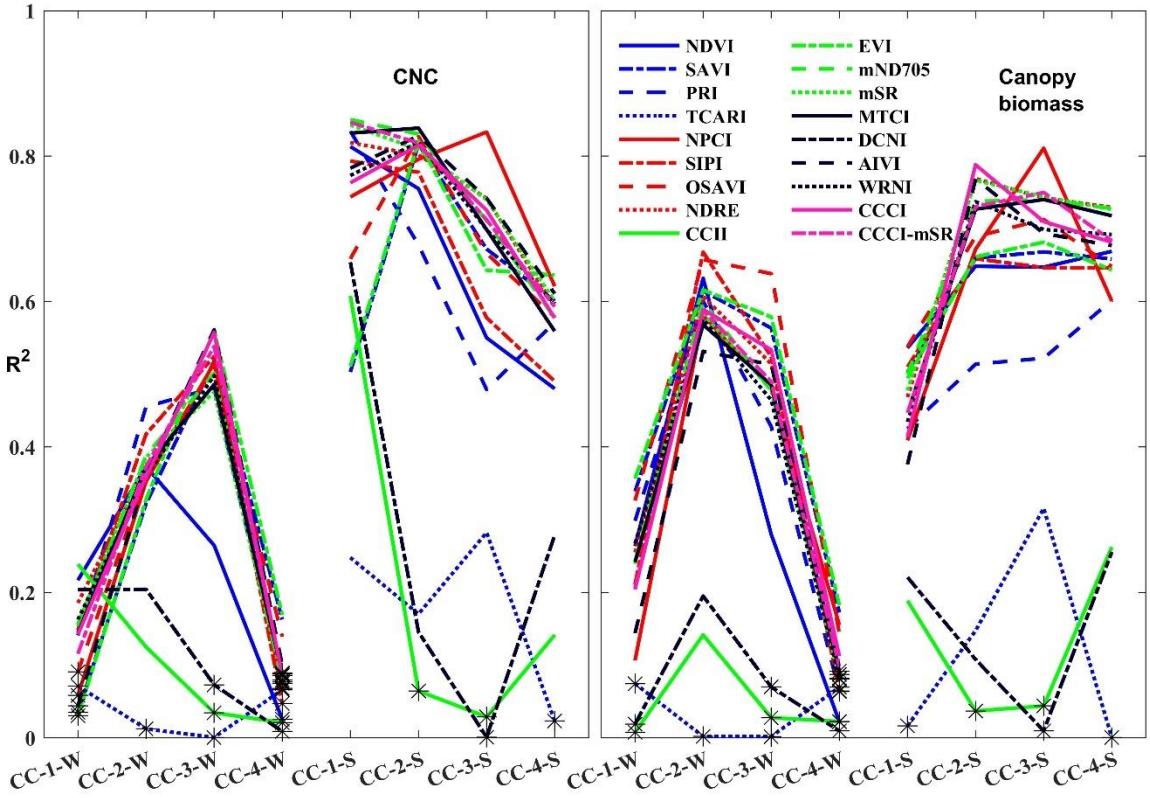

Fig. 6. Coefficient of determination (R^2) for CNC (left panel) and canopy biomass (right panel) at individual growth stages in winter 2018 and summer 2019 (*n*=40). * indicates that the CNC/biomass model did not show statistically significant skills (p >0.05). W and S indicate winter and summer seasons, respectively. The best functional form among L, E, Ll, lL and P relation between spectral indices and crop variables is used to construct the plots. (Double column image, colour)

349 summer CNC assessment. CNC estimation was best for CC-3 in winter and CC-2 in summer
350 (Fig. 7). Compared with CC-3, in winter, the mean NRMSE of spectral indices (except
351 TCARI, CCII and DCNI) was around 27%, 14% and 38% higher for CC-1, 2 and 4

352 respectively. Similarly, CC-2 in summer exhibited the lowest NRMSE in CNC estimation,
353 with NRMSE in CC-1, 3 and 4 being 27%, 24% and 22% higher, respectively.

354 There was a large difference in terms of R^2 and NRMSE in CNC assessment between
355 summer and winter (Fig. 6 and Fig. 7). CNC was much more variable in summer and this
356 primarily led to the higher R^2 values. While raw RMSE was slightly lower in summer, the
357 higher mean CNC in winter (Table 4) led to the lower NRMSE in winter than summer.
358 Although the planar domain indices (CCCI and CCCI-mSR) aim to control for changes in
359 canopy cover when measuring CNC, their association with CNC was similar to the other well-
360 performing indices such as mSR and MTCI (Fig. 6 & Fig. 7).

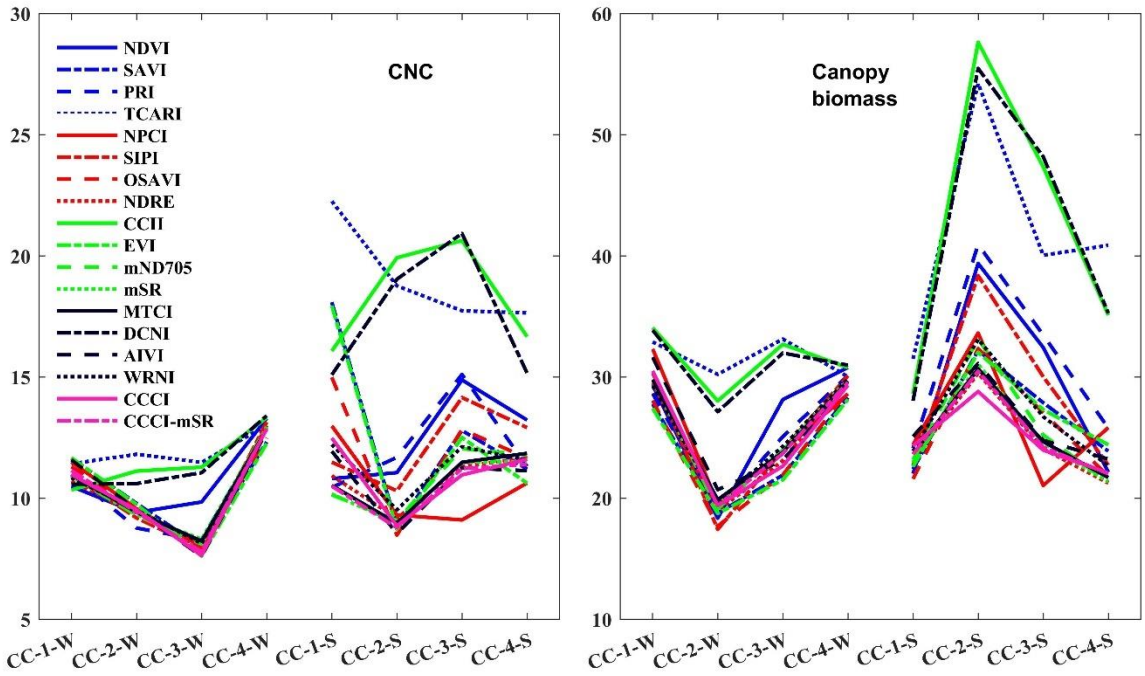

Fig. 7. Corresponding to Fig. 6, normalized RMSE (NRMSE) plots of the remote sensing indices' regression against CNC and canopy biomass in all the individual growth stages in winter 2018 and summer 2019. (Double column image, colour)

361

362 Compared with CNC, the best canopy biomass estimate was shifted towards earlier
363 growth stages – CC-2 (mean NRMSE=21%) in winter and CC-1 (mean NRMSE=25%) in
364 summer (Fig. 7). The NRMSE for canopy biomass showed opposite seasonal patterns;
365 peaking at CC-2 in summer but with the minimum at CC-2 in winter (Fig. 7). As with CNC,
366 the planar domain indices performances in estimating canopy biomass were similar to the
367 conventional one-dimensional indices (e.g. MTCI and AIVI).

368 *3.3. Evaluation of relationship between spectral indices and crop variables across wide range*
369 *of conditions*

370 For the intermediate growth stages, remote sensing indices exhibit moderate to very
371 high performance in estimating CNC and canopy biomass, as shown in Fig. 6. What is not
372 evident from R^2 in Fig. 6 is that the relationships move about over time. This is illustrated
373 using PRI and NPCI in Fig. 8 and Fig. 9, which are typical examples. Plots for the other
374 indices are included in the supplementary information. Thus, the relationship between indices
375 and crop variables established at one growth stage can't be successfully transferred to another
376 growth stage (typical example Fig. 9).

377 To examine whether some indices might be more transferrable between stages, Table
378 5 provides regression summary statistics for the relationship between each spectral index and
379 each of CNC and the perturbing factor, canopy biomass, for pooled data. When all the growth
380 stages were pooled, performance reduced markedly, with only PRI (R^2=0.58) having an R^2
381 greater than 0.26 for CNC. Correlation with biomass also declined markedly, with the best R^2
382 being 0.39 for NPCI.

383 Table 5 also summarises fits to all the data from each season separately. Generally, the
384 RMSE for CNC was similar for summer and winter but the R^2 values for winter are much
385 lower than those for summer as the observed CNC had a lower variance in winter (CV=0.14)
386 (Table 5). In summer, most of the indices were associated with both CNC and canopy

Table 5. Regression statistics between remote sensing indices and crop variables (CNC and canopy biomass) across the seasons (winter 2018 (W), summer 2019 (S) and all seasons together (W+S)). The best out of linear (L), exponential (E), logarithmic-linear (Ll), linear-logarithmic (lL) and power (P) model's RMSE and corresponding coefficient of determination (R^2) values have been listed here.

	CNC (%)						Canopy biomass (kg/ha)					
	R^2			RMSE			R^2			RMSE		
Index	W	S	W+S	W	S	W+S	W	S	W+S	W	S	W+S
NDVI	0.04^{E}	0.29^{E}	0.26^{E}	0.6	0.6	0.9	0.28^{E}	0.50^{lL}	0.26^{E}	460	460	500
SAVI	$\underline{0.00}^{lL}$	0.28^{lL}	0.24^{lL}	0.6	0.6	0.9	0.72^{Ll}	0.41^{E}	0.34^{E}	340	460	470
PRI	$\underline{0.02}^{L}$	$\mathbf{0.77^{Ll}}$	$\mathbf{0.58^{L}}$	0.6	0.3	0.7	0.41^{E}	$\underline{0.01}^{L}$	0.03^{E}	420	600	570
TCARI	0.07^{lL}	$\underline{0.00}^{E}$	0.04^{lL}	0.5	0.7	1.0	0.16^{E}	0.07^{E}	0.07^{E}	500	580	550
NPCI	$\underline{0.00}^{E}$	0.24^{E}	0.13^{E}	0.6	0.6	0.9	0.53^{lL}	0.43^{lL}	$\mathbf{0.39^{lL}}$	370	450	450
SIPI	$\underline{0.02}^{E}$	0.26^{lL}	0.16^{lL}	0.6	0.6	0.9	0.53^{P}	0.51^{P}	0.43^{P}	430	450	470
OSAVI	$\underline{0.01}^{lL}$	0.30^{lL}	0.26^{lL}	0.6	0.6	0.9	0.68^{Ll}	0.43^{E}	0.33^{E}	370	450	470
NDRE	0.03^{lL}	0.40^{lL}	0.17^{lL}	0.6	0.5	0.9	0.40^{E}	$\mathbf{0.47^{E}}$	0.36^{L}	420	440	460
CCII	0.10^{E}	0.08^{lL}	$\underline{0.01}^{E}$	0.5	0.7	1.0	$\underline{0.00}^{lL}$	$\underline{0.01}^{lL}$	$\underline{0.01}^{lL}$	540	600	570
EVI	$\underline{0.00}^{lL}$	0.32^{lL}	0.24^{lL}	0.6	0.6	0.9	$\mathbf{0.60^{E}}$	0.38^{E}	0.34^{E}	340	470	470
mND705	0.03^{lL}	0.45^{E}	0.24^{E}	0.6	0.5	0.9	0.38^{E}	0.38^{E}	0.29^{E}	430	480	490
mSR	0.03^{lL}	0.45^{lL}	0.24^{lL}	0.6	0.5	0.9	0.38^{lL}	0.39^{L}	0.29^{lL}	430	470	490
MTCI	0.03^{lL}	0.49^{lL}	0.24^{lL}	0.6	0.5	0.9	0.38^{lL}	0.36^{L}	0.28^{lL}	430	480	490
DCNI	0.10^{lL}	0.21^{L}	0.05^{L}	0.5	0.6	1.0	$\underline{0.01}^{L}$	$\underline{0.00}^{lL}$	$\underline{0.01}^{lL}$	540	600	570
AIVI	$\underline{0.01}^{lL}$	0.50^{lL}	0.18^{E}	0.6	0.5	0.9	0.41^{lL}	0.33^{E}	0.29^{lL}	420	490	480
WRNI	0.04^{lL}	0.44^{L}	0.18^{E}	0.6	0.5	0.9	0.32^{lL}	0.37^{E}	0.29^{lL}	450	480	480
CCCI	0.03^{lL}	0.42^{lL}	0.13^{E}	0.6	0.5	0.9	0.41^{L}	0.45^{E}	0.37^{L}	420	440	460
CCCI-mSR	0.03^{lL}	0.54^{P}	0.22^{L}	0.6	0.5	0.9	0.38^{L}	0.36^{E}	0.28^{lL}	430	480	490

Sample size (*n*) is 160, 160 and 320 for W, S and W+S respectively. The bolded numbers indicate the best performing index's R^2 with crop variables for the given dataset. Underlined R^2 values indicate $p>0.05$ for the significance of regression slope.

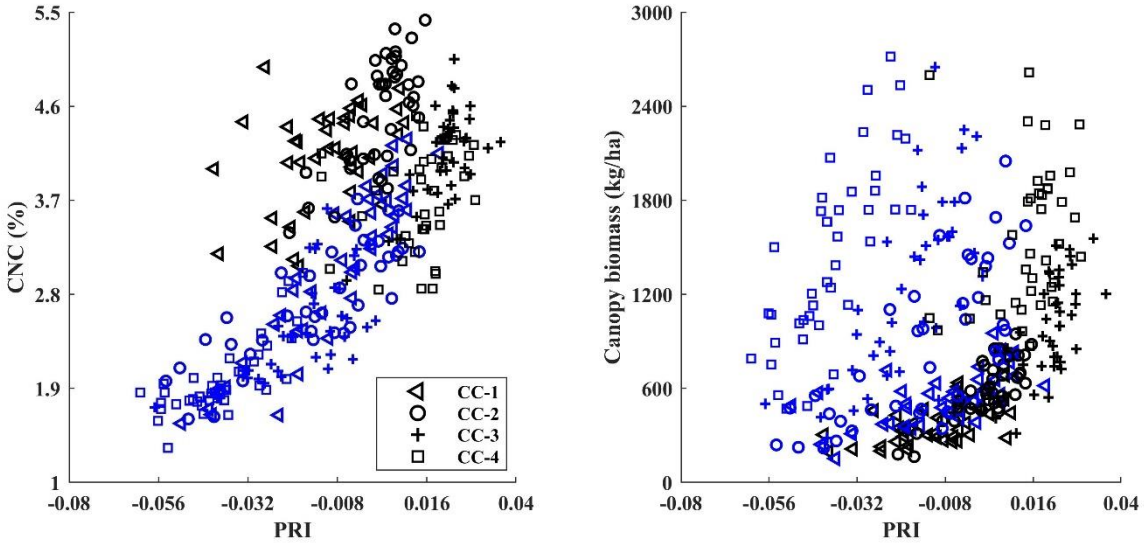

Fig. 8. Relationship between PRI and CNC and canopy biomass in winter (black) and summer (blue) at each growth stage. (Double column fitting image, colour)

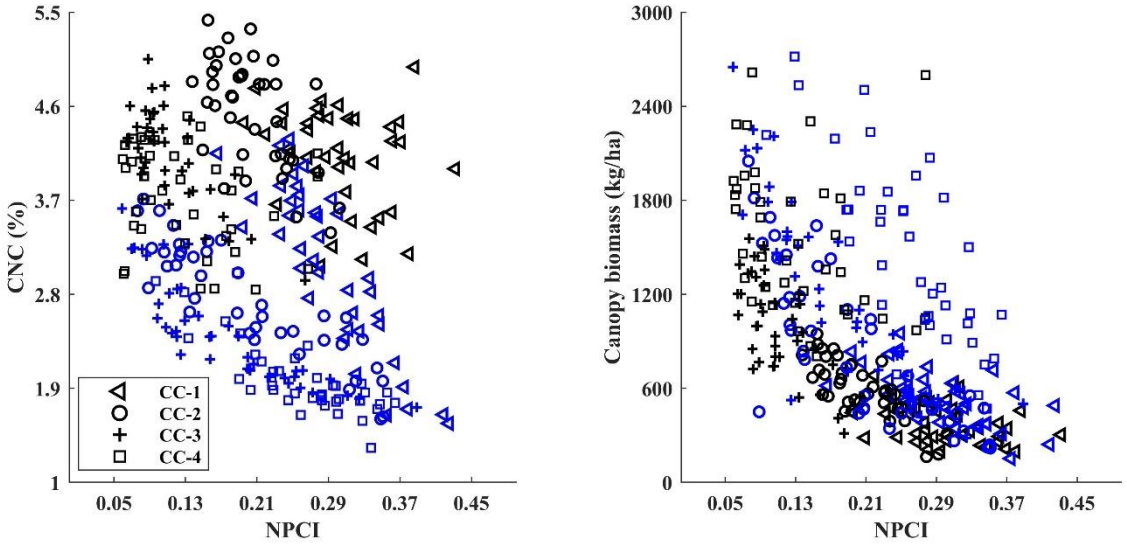

Fig. 9. Relationship between NPCI and CNC and canopy biomass in winter (black) and summer (blue) at each growth stage. (Double column image, colour)

biomass; the exceptions being PRI, DCNI, CCII and TCARI. In contrast to CNC, association with biomass were generally better in winter than summer, both in terms of R^2 and RMSE.

PRI is best correlated with CNC, with R^2=0.77 and RMSE=0.3% in summer 2019, and

R^2=0.58 and RMSE=0.7% overall, with effectively no correlation with canopy biomass (R^2=0.01). In winter, PRI had a poor relationship with CNC but an R^2 of 0.41 for canopy biomass (Table 5). Fig. 8 shows the relationship of PRI with CNC and canopy biomass across all the data with growth stages and seasons identified. There is wide scatter at individual growth stages (particularly at CC-1 and 2 in winter), but a consistent relationship when all stages are combined. PRI's relationship with canopy biomass shifted with growth stage and season, leading to particularly high RMSE and significant scatter in summer (Table 5 and Fig. 8).

Despite nominally controlling for changes in canopy cover confounding canopy N signals, the planar domain indices were poor at representing CNC (Table 5). Furthermore, overall, they were actually more sensitive (higher R^2) to canopy biomass than CNC (Table 5). CCCI-mSR's performance was slightly better than CCCI in CNC estimation.

Unlike CNC estimation, no single standout spectral index was found for estimating canopy biomass. There were many candidate indices with relatively better sensitivity towards canopy biomass (e.g. EVI, SAVI, OSAVI, NDRE, CCCI, NPCI showed similar performance) in winter, summer and pooled data. RMSE increased for all spectral indices, especially SAVI, PRI, NPCI, OSAVI and EVI, when estimating canopy biomass during summer compared with winter (Table 5). EVI and NDRE exhibited better performance in estimating canopy biomass in winter and summer, respectively (Table 5). However, when a wide range of conditions were pooled together, NPCI was the most robust and accurate. Most of the spectral indices (except for TCARI, CCII and DCNI) were only slightly to moderately correlated with canopy biomass in the pooled dataset. Wider scatter was observed at CC-4 in both winter and summer for the relationship between NPCI, CNC and canopy biomass (Fig. 9). This high scatter was also evident with other spectral indices at CC-4 in both seasons (see supplementary information for plots).

Saturation was observed for spectral indices such as NDVI and SIPI for both CNC and canopy biomass (see supplementary information for plots). As with the results for individual days (season and growth stage), TCARI, CCII and DCNI did not respond to either CNC or canopy biomass. Moreover, fWBI (used in estimating WRNI in this study) (Strachan et al., 2002) had the highest and most consistent correlation with canopy biomass in both seasons and collectively (R^2= 0.64, 0.66, 0.55; RMSE= 360, 320, 390 kg/ha, respectively for winter, summer and pooled data).

4. Discussion

This study aimed to evaluate the performance of selected spectral indices for sensing CNC across a wide range of growth and environmental conditions, as well as to evaluate the influence of canopy biomass on CNC estimation. The most important finding that emerges from the results is that the relationship between various spectral indices and CNC changes between growth stages and seasons (Fig. 6 and a typical example Fig. 9). Therefore, the correlation between CNC and individual indices varied significantly across growth stages and seasons. This finding is consistent with those of Feng et al. (2016) (wheat), Gitelson et al. (2017) (soybean and maize) and Li et al. (2014a) (maize) who found different relationships between the indices they considered and canopy properties (N and chlorophyll) at different growth stages. As a consequence of this changing relationship, the correlation between individual indices and CNC declines markedly when evaluated against the pooled data (Table 5) for nearly all indices. Moreover, many of the indices previously reported as CNC indicators responded to both CNC and canopy biomass (Table 5 and Fig. 6). Fig. 6 shows that most of the indices have similar sensitivity to changes in CNC and canopy biomass. Spectral indices are influenced by many factors including biomass, soil background, canopy structure and environmental variables (Cammarano et al., 2014; Govaerts et al., 1999; Hansen and Schjoerring, 2003), with biomass being the most significant (Stroppiana et al., 2009). Thus,

designing an index sensitive to only one target variable (e.g. CNC here) has been challenging and a prime focus of the remote sensing community. In most previous CNC sensing studies, indices were evaluated or developed with data from a limited range of growth stages and seasons. An implication of our results is that future research on developing indices less influenced by biomass and showing consistent sensitivity to CNC should focus on incorporating a comprehensive range of growth and environmental conditions.

In addition, caution should be used when designing/modifying indices for CNC mapping at the canopy scale. As can be seen from Fig. 5, certain growth stages have a high correlation between ground CNC and canopy biomass (as high as 0.90). This high correlation may confound the retrieval of canopy scale CNC signals that are distinct from the biomass effects. The susceptibility to biomass attributes of canopy level indices further adds complexity in retrieving distinct CNC signals (Daughtry et al., 2000; Haboudane et al., 2002; Stroppiana et al., 2009; Yoder and Pettigrew-Crosby, 1995) and the sensitivity of some indices at certain growth stages to CNC may be only applicable to the extent that CNC and canopy biomass are correlated. Moreover, incorporating a wide range of N application treatments brings more scatter to the CNC-biomass relation (Fig 4c,d). One possible implication is that under relatively homogenous N treatments or certain soil-plant interactions, CNC-biomass may be negatively correlated across growth stages (due to the CNC dilution). Therefore, indices significantly influenced by biomass may perform better for CNC sensing to the extent this correlation holds. Thus, it could be argued that even across growth stages, performance of spectral indices may not be a decisive test of its sensitivity to CNC.

While we found poor performance from many indices when confronted with a range of growth stages, PRI performed quite well. PRI was originally designed with the aim of sensing the xanthophyll cycle and has been related with many canopy properties such as photosynthetic light use efficiency (LUE) (Barton and North, 2001; Gamon et al., 1992;

Goerner et al., 2009; Jia et al., 2018), chlorophyll : carotenoid ratio (Gamon et al., 2015) and LAI (Gitelson et al., 2017). Depending on the temporal scale of measurements, the stronger relationship switches between LUE and the chlorophyll : carotenoids ratio (Gamon et al., 2015). Nevertheless, among the 18 spectral indices evaluated, PRI showed the best and most consistent performance in monitoring CNC (Table 5). PRI has not been explicitly recognized as a CNC indicator in the literature, but some recent studies have also reported moderate to high association of PRI with CNC for wheat (He et al., 2016; Ranjan et al., 2012), rice (Tian et al., 2011) and barley (Xu et al., 2014). PRI's positive relation with chlorophyll : carotenoids ratio and chlorophyll content at the seasonal timescale (Gamon et al., 2015; Gitelson et al., 2017), together with the functional relation between chlorophyll and CNC likely explains the robust performance of canopy level PRI for CNC here. While PRI showed the greatest consistency with CNC, the relationship deviated at the lowest canopy covering growth stage (CC-1 winter), which is consistent with the findings of soil influence by Barton and North (2001) (Fig. 8).

When considering each season separately, PRI yielded a moderate correlation with canopy biomass in winter and no relationship in summer, and vice versa for CNC (Table 5). PRI has multiple drivers at canopy level, one of which is LAI (Barton and North, 2001; Gitelson et al., 2017). Together with low photoprotection (xanthophyll cycle) activity during winter, this might explain the enhanced correlation between PRI and canopy biomass that appeared only in winter. This seasonal association of PRI with biomass affects its ability to estimate CNC across the seasons. Thus, the coefficient of determination (R^2) dropped from 0.77 in summer to 0.58 in the pooled data (Table 5). Considering the conflicting conclusions by Gamon et al. (2015), Gitelson et al. (2017) and Sims and Gamon (2002) together with a lack of ground LUE or chlorophyll : carotenoid ratio data, it remains unclear why PRI was related to CNC in summer but to canopy biomass in winter. Further studies investigating

PRI's changing relationship with canopy biomass and CNC over the different seasons are needed.

Another key issue in this study is that the spectral indices designed for CNC/chlorophyll actually performed better for sensing canopy biomass. The performance of most of the indices was also more consistent for canopy biomass than CNC, even in the pooled dataset (Table 5), suggesting that a significant amount of the variability in the canopy level indices comes from canopy biomass. Daughtry et al. (2000) also reported a very significant proportion (>90%) of variability in the spectral indices attributed to LAI. Like Viña et al. (2011) for maize and soybean, we found that EVI and MTCI more consistently represent canopy biomass. Zarate-Valdez et al. (2012) also reported the same for EVI from the almond crop. NDVI and SIPI showed (results in supplementary material) early saturation, compared with other indices. We also found that NPCI, SAVI, OSAVI, EVI, NDRE are more consistently related to canopy biomass (Table 5). In accordance with our results, previous studies have also demonstrated saturation of NDVI at high biomass level (Stroppiana et al., 2009) in rice and Viña et al. (2011) in maize and soybean). Contrary to the results of He et al. (2016) on AIVI (developed on wheat), we found it more consistent with canopy biomass than CNC in ryegrass (Table 5).

The relationship between spectral indices and canopy biomass exhibits most scatter at the highest biomass stages, in contrast to CNC where the early growth stages (lower biomass) show more scatter (Fig. 8 and Fig. 9). This is likely due to a) saturation for high biomass and b) the influence of visible soil at low biomass. Saturation at high biomass is common in canopy remote sensing (Haboudane et al., 2004; Serrano et al., 2000; Strachan et al., 2002; Schlemmer et al., 2013; Viña et al., 2011), while the significant influence of soil background on the inference of CNC from spectral indices was discussed by Bausch (1993), Daughtry et al. (2000) and Huete (1988). Bausch (1993) (corn) and Flowers et al. (2003) (wheat)

515 demonstrated that NDVI was significantly affected by the soil background reflectance.
516 Furthermore, Flowers et al. (2003) found that adequate above-ground biomass is required
517 when mapping wheat N using spectral indices.

518 Recognizing the impact of canopy cover on CNC detection, Barnes et al. (2000)
519 proposed CCCI. We found a weaker association between planar domain indices (CCCI and
520 CCCI-mSR) and CNC than between some other indices such as PRI and CNC, both in
521 seasonal and pooled data (Table 5). This contradicts CCCI results reported by Fitzgerald et al.
522 (2010), Li et al. (2014a, 2014b), Rodriguez et al. (2006) and Tilling et al. (2007) in wheat;
523 Barnes et al. (2000), El-Shikha et al. (2008) in cotton; Li et al. (2014a) in maize; and Varco et
524 al. (2013) in cotton and maize. Each of those studies was limited to certain growth stages
525 and/or less diverse N fertiliser application conditions, which likely explains this. Our results
526 support findings from Cammarano et al. (2014), El-Shikha et al. (2008), Li et al. (2014a) and
527 Tilling et al. (2007) who found that CCCI performance decreased when evaluated across
528 growth stages. Finally, while planar domain indices have been found to improve CNC
529 detection at low canopy cover compared with other indices (El-Shikha et al., 2008), this was
530 not the case at CC-1 in this study (Fig. 6).

531 The relationship between CCCI and biomass is also interesting to consider. CCCI
532 nominally controls for canopy cover, which is related to biomass; however, we found a
533 stronger relationship between CCCI and biomass than CCCI and CNC. It is likely that the
534 correlation between CNC and canopy biomass (Fig. 5) is driving the stage specific
535 relationship between CCCI and CNC. The relationship between CCCI, LAI and biomass
536 observed by Cammarano et al. (2014) and Li et al. (2014b) corroborate our findings of a more
537 consistent association between CCCI and canopy biomass than CNC, and CNC-CCCI
538 relationship may be applicable to the limit that biomass-CNC are correlated.

539 In applying remote sensing to assess canopy N status, both CNC and N uptake have

been used. Many previous remote sensing studies have used N uptake as a N status diagnosis tool (Cammarano et al., 2014; Clevers and Gitelson, 2013; Clevers and Kooistra, 2011; Fitzgerald et al., 2010; Guo et al., 2017; Hansen and Schjoerring, 2003; Li et al., 2014b; Schlemmer et al., 2013); however, there is often a strong correlation between canopy biomass and N uptake ($0.86<r<0.99$ here), indicating that N uptake and canopy biomass measurements are not independent of each other (Fig. 5). Moreover, there is some value to this in an environment where N application is uniform. Then N uptake might reflect (negatively correlate with) remaining N availability. This implicitly assumes other N loss processes are either minor or spatially uniform, which is unlikely in many landscapes. Reinforcing the potential issues of relying on N update, Chen et al. (2010) reported that NNI calculation from CNC is more accurate than using N uptake. The remote sensing issue here is that any spectral index sensitive to canopy biomass is also likely to be sensitive to canopy N uptake but may have the limited skill in predicting CNC.

Another important issue is the transferability of spectral indices or models based on specific spectral indices across crop types. Some indices developed on different crops are performing poorly here in ryegrass. Useful relationships have been found with CNC for CCII (Haboudane et al., 2002) in corn, DCNI (Chen et al., 2010), TCARI (Haboudane et al., 2008) in corn and wheat, NDRE (Barnes et al., 2000) in cotton, NPCI (Peñuelas et al., 1994) in sunflower leaves and AIVI (He et al., 2016) in wheat; but we did not find any agreement between these indices and CNC. This is probably due to idiosyncrasies of spectral responses for different crop types. It is likely that the difference in the position of highly correlated bands of CNC between crop types have lowered the sensitivity of these indices (Shi et al., 2015). Haboudane et al. (2008) have even shown clear differences in the prediction power of indices in wheat and corn with the same chlorophyll content range.

Another source of uncertainty in index performance is optical remote sensing's operational linkage to CNC, which derives from its correlation with chlorophyll. This correlation is not consistent and robust across the species (Berger et al., 2020; Hallik et al., 2009; Homolova et al., 2013). N taken up by the plants is not only insignificantly invested in chlorophyll compounds but distributed among other nonphotochemical proteins, which may alter the relationship between chlorophyll and CNC and, ultimately, the predictive performance of spectral indices from one species to another (Berger et al., 2020).

The fact that most indices are sensitive to both CNC and canopy biomass (Fig. 6 and Table 5) raises an important question of finding a band combination that is best suited to estimating CNC at canopy level with minimal interference from other biophysical and environmental factors. One possible way to identify spectral indices that are sensitive to CNC and robust across a contrasting range of canopy biomass and seasonal conditions is to couple hyperspectral reflectance data with a data mining approach. This could consist of an exhaustive search of all band combinations in some general spectral index formula (e.g. Yao et al. (2014)). In such future investigations, it is important to consider the CNC-biomass correlation.

Despite using contrasting growth stages and seasons, it should be noted that the above findings are drawn from irrigated ryegrass pasture, and therefore the fidelity and generalizability of this work need further investigation using more diverse crop types and agroecological environments. CNC and chlorophyll relations are likely to be species dependent. Currently, it is not clear to what extent a uniform approach across species is practical, and there needs to be more cross-species comparisons to investigate this. The confounding effects of multiple stress factors such as water stress and a range of other macro- and micro-nutrients may also alter the plant function and consequently, the relationship between spectral indices and CNC.

5. Conclusion

CNC information from remote sensing platforms with suitable spatial and temporal resolutions can potentially improve the efficiency of N fertilisation and the economic output of farms and reduce environmental impacts of excess N fertiliser application. For the remotely sensed CNC to be adopted in practice, the spectral index used should have sufficient sensitivity to CNC across a variety of environmental conditions and be independent of confounding factors such as biomass. This paper uses field data for ryegrass under a range of N treatments and a variety of growth stages and seasons to examine the performance of eighteen existing spectral indices for sensing CNC and canopy biomass. It particularly considers the interaction between biomass and CNC.

The following conclusions can be drawn from this study.

1. For most of the indices considered, the relationship of MS indices with CNC varied between individual growth stages. Therefore, their performance reduced greatly when applied to pooled data. Furthermore, some growth stages have a high correlation between CNC and canopy biomass. This can lead to biomass sensitive indices being a good CNC indicator at those times but to inconsistent performance between growth stages. Therefore, the selection of remote sensing indices should be based on a wide range of conditions, not just individual growth stages or seasons. Using a wide range of conditions can lead to a more reliable selection of a spectral index for CNC sensing applicable to a variety of conditions.

2. PRI showed the best correlation with CNC when assessed across a contrasting range of conditions. Nevertheless, environmental variables can shift the relationship of PRI with CNC and canopy biomass.

3. Planar domain indices did not exhibit superior skill in CNC estimation compared with conventional spectral indices, including at the lowest canopy cover stages (CC-1).

4. Most of the indices showed correlation with CNC, though the correlation and relationship were dependent on specific growth conditions.

5. Given that the eighteen indices considered responded to both CNC and canopy biomass, further studies separating CNC and biomass signals are needed to develop more broadly applicable CNC models.

Acknowledgments

This work was supported by the Australian Government Department of Agriculture, Water and the Environment as part of its Rural R&D for Profit program (grant No. RRDP1715); the Australia-China Joint Research Centre for Healthy Soils for Sustainable Food Production and Environmental Quality (grant No. ACSRF48165); and Dairy Australia. We are thankful to Dr. Alexis Pang, Mr. Graeme Ward and Dr. Oxana Belyaeva who helped in maintaining the crop condition and organising the ground data collection. The authors would also like to acknowledge the timely services provided by TrACEES platform in chemical analysis at the University of Melbourne.

Conflicts of Interest

The authors declare no conflict of interest.

References

Asner, G.P., 1998. Biophysical and biochemical sources of variability in canopy reflectance. Remote Sens. Environ. 64, 234–253.

Baret, F., Fourty, T., 1997. Radiometric estimates of nitrogen status of leaves and canopies, in: Diagnosis of the Nitrogen Status in Crops. Springer, pp. 201–227.

Barnes, E.M., Clarke, T.R., Richards, S.E., Colaizzi, P.D., Haberland, J., Kostrzewski, M., Waller, P., Choi C., R.E., Thompson, T., Lascano, R.J., Li, H., Moran, M.S., 2000.

637 Coincident detection of crop water stress, nitrogen status and canopy density using ground
638 based multispectral data, in: Proc. 5th Int. Conf. Precis Agric. pp. 1–15.

639 Barton, C.V.M., North, P.R.J., 2001. Remote sensing of canopy light use efficiency using the
640 photochemical reflectance index: Model and sensitivity analysis. Remote Sens. Environ.
641 78, 264–273.

642 Basso, B., Fiorentino, C., Cammarano, D., Schulthess, U., 2016. Variable rate nitrogen fertilizer
643 response in wheat using remote sensing. Precis. Agric. 17, 168–182.

644 Bausch, W.C., 1993. Soil background effects on reflectance-based crop coefficients for corn.
645 Remote Sens. Environ. 46, 213–222.

646 Berger, K., Verrelst, J., Féret, J.-B., Wang, Z., Wocher, M., Strathmann, M., Danner, M.,
647 Mauser, W., Hank, T., 2020. Crop nitrogen monitoring: Recent progress and principal
648 developments in the context of imaging spectroscopy missions. Remote Sens. Environ.
649 242, 111758.

650 Cammarano, D., Fitzgerald, G.J., Casa, R., Basso, B., 2014. Assessing the robustness of
651 vegetation indices to estimate wheat N in Mediterranean environments. Remote Sens. 6,
652 2827–2844.

653 Chen, P., Haboudane, D., Tremblay, N., Wang, J., Vigneault, P., Li, B., 2010. New spectral
654 indicator assessing the efficiency of crop nitrogen treatment in corn and wheat. Remote
655 Sens. Environ. 114, 1987–1997.

656 Clarke, T.R., Moran, M.S., Barnes, E.M., Pinter, P.J., Qi, J., 2001. Planar domain indices: A
657 method for measuring a quality of a single component in two-component pixels, in:
658 IGARSS 2001. Scanning the Present and Resolving the Future. Proceedings. IEEE 2001
659 International Geoscience and Remote Sensing Symposium (Cat. No. 01CH37217). IEEE,

660 pp. 1279–1281.

661 Clevers, J.G.P.W., Gitelson, A.A., 2013. Remote estimation of crop and grass chlorophyll and
662 nitrogen content using red-edge bands on Sentinel-2 and-3. Int. J. Appl. Earth Obs. Geoinf.
663 23, 344–351.

664 Clevers, J.G.P.W., Kooistra, L., 2011. Using hyperspectral remote sensing data for retrieving
665 canopy chlorophyll and nitrogen content. IEEE J. Sel. Top. Appl. earth Obs. Remote Sens.
666 5, 574–583.

667 Curran, P.J., 1989. Remote sensing of foliar chemistry. Remote Sens. Environ. 30, 271–278.

668 Dash, J., Curran, P.J., 2004. The MERIS terrestrial chlorophyll index. Int. J. Remote Sens. 25,
669 5403–5413.

670 Daughtry, C.S.T., Walthall, C.L., Kim, M.S., De Colstoun, E.B., McMurtrey Iii, J.E., 2000.
671 Estimating corn leaf chlorophyll concentration from leaf and canopy reflectance. Remote
672 Sens. Environ. 74, 229–239.

673 El-Shikha, D.M., Barnes, E.M., Clarke, T.R., Hunsaker, D.J., Haberland, J.A., Pinter Jr, P.J.,
674 Waller, P.M., Thompson, T.L., 2008. Remote sensing of cotton nitrogen status using the
675 canopy chlorophyll content index (CCCI). Trans. ASABE 51, 73–82.

676 El-Shikha, D.M., Waller, P., Hunsaker, D., Clarke, T., Barnes, E., 2007. Ground-based remote
677 sensing for assessing water and nitrogen status of broccoli. Agric. water Manag. 92, 183–
678 193.

679 Feng, W., Zhang, H.-Y., Zhang, Y.-S., Qi, S.-L., Heng, Y.-R., Guo, B.-B., Ma, D.-Y., Guo, T.-
680 C., 2016. Remote detection of canopy leaf nitrogen concentration in winter wheat by using
681 water resistance vegetation indices from in-situ hyperspectral data. F. Crop. Res. 198, 238–
682 246.

683 Fitzgerald, G., Rodriguez, D., O'Leary, G., 2010. Measuring and predicting canopy nitrogen
684 nutrition in wheat using a spectral index—The canopy chlorophyll content index (CCCI).
685 F. Crop. Res. 116, 318–324.

686 Fitzgerald, G.J., Rodriguez, D., Christensen, L.K., Belford, R., Sadras, V.O., Clarke, T.R.,
687 2006. Spectral and thermal sensing for nitrogen and water status in rainfed and irrigated
688 wheat environments. Precis. Agric. 7, 233–248.

689 Flowers, M., Weisz, R., Heiniger, R., 2003. Quantitative approaches for using color infrared
690 photography for assessing in-season nitrogen status in winter wheat. Agron. J. 95, 1189–
691 1200.

692 Fourty, T., Baret, F., Jacquemoud, S., Schmuck, G., Verdebout, J., 1996. Leaf optical properties
693 with explicit description of its biochemical composition: direct and inverse problems.
694 Remote Sens. Environ. 56, 104–117.

695 Gabriel, J.L., Zarco-Tejada, P.J., López-Herrera, P.J., Pérez-Martín, E., Alonso-Ayuso, M.,
696 Quemada, M., 2017. Airborne and ground level sensors for monitoring nitrogen status in
697 a maize crop. Biosyst. Eng. 160, 124–133.

698 Gamon, J.A., Kovalchuck, O., Wong, C.Y.S., Harris, A., Garrity, S.R., 2015. Monitoring
699 seasonal and diurnal changes in photosynthetic pigments with automated PRI and NDVI
700 sensors. Biogeosciences 12.

701 Gamon, J.A., Penuelas, J., Field, C.B., 1992. A narrow-waveband spectral index that tracks
702 diurnal changes in photosynthetic efficiency. Remote Sens. Environ. 41, 35–44.

703 Gitelson, A.A., Gamon, J.A., Solovchenko, A., 2017. Multiple drivers of seasonal change in
704 PRI: Implications for photosynthesis 2. Stand level. Remote Sens. Environ. 190, 198–206.

705 Goerner, A., Reichstein, M., Rambal, S., 2009. Tracking seasonal drought effects on ecosystem

light use efficiency with satellite-based PRI in a Mediterranean forest. Remote Sens. Environ. 113, 1101–1111.

Govaerts, Y.M., Verstraete, M.M., Pinty, B., Gobron, N., 1999. Designing optimal spectral indices: A feasibility and proof of concept study. Int. J. Remote Sens. 20, 1853–1873.

Guo, B.-B., Qi, S.-L., Heng, Y.-R., Duan, J.-Z., Zhang, H.-Y., Wu, Y.-P., Feng, W., Xie, Y.-X., Zhu, Y.-J., 2017. Remotely assessing leaf N uptake in winter wheat based on canopy hyperspectral red-edge absorption. Eur. J. Agron. 82, 113–124.

Gupta, R.K., Mostaghimi, S., McClellan, P.W., Alley, M.M., Brann, D.E., 1997. Spatial variability and sampling strategies for NO3-N, P, and K determinations for site-specific farming. Trans. ASAE 40, 337–343.

Haboudane, D., Miller, J.R., Pattey, E., Zarco-Tejada, P.J., Strachan, I.B., 2004. Hyperspectral vegetation indices and novel algorithms for predicting green LAI of crop canopies: Modeling and validation in the context of precision agriculture. Remote Sens. Environ. 90, 337–352.

Haboudane, D., Miller, J.R., Tremblay, N., Zarco-Tejada, P.J., Dextraze, L., 2002. Integrated narrow-band vegetation indices for prediction of crop chlorophyll content for application to precision agriculture. Remote Sens. Environ. 81, 416–426.

Haboudane, D., Tremblay, N., Miller, J.R., Vigneault, P., 2008. Remote estimation of crop chlorophyll content using spectral indices derived from hyperspectral data. IEEE Trans. Geosci. Remote Sens. 46, 423–437.

Hallik, L., Kull, O., Niinemets, Ü., Aan, A., 2009. Contrasting correlation networks between leaf structure, nitrogen and chlorophyll in herbaceous and woody canopies. Basic Appl. Ecol. 10, 309–318.

729 Hank, T.B., Berger, K., Bach, H., Clevers, J.G.P.W., Gitelson, A., Zarco-Tejada, P., Mauser,
730 W., 2019. Spaceborne imaging spectroscopy for sustainable agriculture: Contributions and
731 challenges. Surv. Geophys. 40, 515–551.

732 Hansen, P.M., Schjoerring, J.K., 2003. Reflectance measurement of canopy biomass and
733 nitrogen status in wheat crops using normalized difference vegetation indices and partial
734 least squares regression. Remote Sens. Environ. 86, 542–553.

735 He, L., Song, X., Feng, W., Guo, B.-B., Zhang, Y.-S., Wang, Y.-H., Wang, C.-Y., Guo, T.-C.,
736 2016. Improved remote sensing of leaf nitrogen concentration in winter wheat using multi-
737 angular hyperspectral data. Remote Sens. Environ. 174, 122–133.

738 Homolova, L., Malenovský, Z., Clevers, J.G.P.W., García-Santos, G., Schaepman, M.E., 2013.
739 Review of optical-based remote sensing for plant trait mapping. Ecol. Complex. 15, 1–16.

740 Huete, A., 1988. A soil-adjusted vegetation index (SAVI). Remote Sens. Environ. 25, 295–309.

741 Huete, A., Didan, K., Miura, T., Rodriguez, E.P., Gao, X., Ferreira, L.G., 2002. Overview of
742 the radiometric and biophysical performance of the MODIS vegetation indices. Remote
743 Sens. Environ. 83, 195–213.

744 Jay, S., Maupas, F., Bendoula, R., Gorretta, N., 2017. Retrieving LAI, chlorophyll and nitrogen
745 contents in sugar beet crops from multi-angular optical remote sensing: Comparison of
746 vegetation indices and PROSAIL inversion for field phenotyping. F. Crop. Res. 210, 33–
747 46.

748 Jia, W., Coops, N.C., Tortini, R., Pang, Y., Black, T.A., 2018. Remote sensing of variation of
749 light use efficiency in two age classes of Douglas-fir. Remote Sens. Environ. 219, 284–
750 297.

751 Kim, M.S., Daughtry, C.S.T., Chappelle, E.W., McMurtrey III, J.E., Walthall, C.L., 1994. The

752 use of high spectral resolution bands for estimating absorbed photosynthetically active
753 radiation (Apar). Proc. 6th Symp. Phys. Meas. Signatures Remote Sens. 299–306.

754 Lamb, D.W., Steyn-Ross, M., Schaare, P., Hanna, M.M., Silvester, W., Steyn-Ross, A., 2002.
755 Estimating leaf nitrogen concentration in ryegrass (Lolium spp.) pasture using the
756 chlorophyll red-edge: theoretical modelling and experimental observations. Int. J. Remote
757 Sens. 23, 3619–3648.

758 Lemaire, G., Jeuffroy, M.-H., Gastal, F., 2008. Diagnosis tool for plant and crop N status in
759 vegetative stage: Theory and practices for crop N management. Eur. J. Agron. 28, 614–
760 624.

761 Li, F., Miao, Y., Feng, G., Yuan, F., Yue, S., Gao, X., Liu, Y., Liu, B., Ustin, S.L., Chen, X.,
762 2014a. Improving estimation of summer maize nitrogen status with red edge-based
763 spectral vegetation indices. F. Crop. Res. 157, 111–123.

764 Li, F., Miao, Y., Hennig, S.D., Gnyp, M.L., Chen, X., Jia, L., Bareth, G., 2010. Evaluating
765 hyperspectral vegetation indices for estimating nitrogen concentration of winter wheat at
766 different growth stages. Precis. Agric. 11, 335–357.

767 Li, F., Mistele, B., Hu, Y., Chen, X., Schmidhalter, U., 2014b. Optimising three-band spectral
768 indices to assess aerial N concentration, N uptake and aboveground biomass of winter
769 wheat remotely in China and Germany. ISPRS J. Photogramm. Remote Sens. 92, 112–
770 123.

771 Mamo, M., Malzer, G.L., Mulla, D.J., Huggins, D.R., Strock, J., 2003. Spatial and temporal
772 variation in economically optimum nitrogen rate for corn. Agron. J. 95, 958–964.

773 Matejovic, I., 1995. Total nitrogen in plant material determinated by means of dry combustion:
774 A possible alternative to determination by Kjeldahl digestion. Commun. Soil Sci. Plant

775 Anal. 26, 2217–2229.

776 Mosier, A., Kroeze, C., Nevison, C., Oenema, O., Seitzinger, S., Van Cleemput, O., 1998.
777 Closing the global N 2 O budget: nitrous oxide emissions through the agricultural nitrogen
778 cycle. Nutr. Cycl. Agroecosystems 52, 225–248.

779 Penuelas, J., Baret, F., Filella, I., 1995. Semi-empirical indices to assess
780 carotenoids/chlorophyll a ratio from leaf spectral reflectance. Photosynthetica 31, 221–
781 230.

782 Peñuelas, J., Gamon, J.A., Fredeen, A.L., Merino, J., Field, C.B., 1994. Reflectance indices
783 associated with physiological changes in nitrogen- and water-limited sunflower leaves.
784 Remote Sens. Environ. 48, 135–146. https://doi.org/10.1016/0034-4257(94)90136-8

785 Perry, E.M., Fitzgerald, G.J., Nuttall, J.G., O'Leary, G.J., Schulthess, U., Whitlock, A., 2012.
786 Rapid estimation of canopy nitrogen of cereal crops at paddock scale using a Canopy
787 Chlorophyll Content Index. F. Crop. Res. 134, 158–164.

788 Plénet, D., Lemaire, G., 1999. Relationships between dynamics of nitrogen uptake and dry
789 matter accumulation in maize crops. Determination of critical N concentration. Plant Soil
790 216, 65–82.

791 Ranjan, R., Chopra, U.K., Sahoo, R.N., Singh, A.K., Pradhan, S., 2012. Assessment of plant
792 nitrogen stress in wheat (Triticum aestivum L.) through hyperspectral indices. Int. J.
793 Remote Sens. 33, 6342–6360.

794 Reich, P.B., Oleksyn, J., 2004. Global patterns of plant leaf N and P in relation to temperature
795 and latitude. Proc. Natl. Acad. Sci. 101, 11001–11006.

796 Rodriguez, D., Fitzgerald, G.J., Belford, R., Christensen, L.K., 2006. Detection of nitrogen
797 deficiency in wheat from spectral reflectance indices and basic crop eco-physiological

798 concepts. Aust. J. Agric. Res. 57, 781–789. https://doi.org/10.1071/AR05361

799 Rondeaux, G., Steven, M., Baret, F., 1996. Optimization of soil-adjusted vegetation indices.
800 Remote Sens. Environ. 55, 95–107.

801 Rouse, J.W., Haas, R.H., Schell, J.A., Deering, D.W., 1973. Monitoring vegetation systems in
802 the Great Plains with ERTS. Proc. 3rd ERTS Symp. 1, 309–317.

803 Schlemmer, M., Gitelson, A., Schepers, J., Ferguson, R., Peng, Y., Shanahan, J., Rundquist, D.,
804 2013. Remote estimation of nitrogen and chlorophyll contents in maize at leaf and canopy
805 levels. Int. J. Appl. Earth Obs. Geoinf. 25, 47–54.

806 Serrano, L., Filella, I., Penuelas, J., 2000. Remote sensing of biomass and yield of winter wheat
807 under different nitrogen supplies. Crop Sci. 40, 723–731.

808 Shi, T., Wang, J., Liu, H., Wu, G., 2015. Estimating leaf nitrogen concentration in
809 heterogeneous crop plants from hyperspectral reflectance. Int. J. Remote Sens. 36, 4652–
810 4667.

811 Sims, D.A., Gamon, J.A., 2002. Relationships between leaf pigment content and spectral
812 reflectance across a wide range of species, leaf structures and developmental stages.
813 Remote Sens. Environ. 81, 337–354. https://doi.org/10.1016/S0034-4257(02)00010-X

814 Strachan, I.B., Pattey, E., Boisvert, J.B., 2002. Impact of nitrogen and environmental conditions
815 on corn as detected by hyperspectral reflectance. Remote Sens. Environ. 80, 213–224.

816 Stroppiana, D., Boschetti, M., Brivio, P.A., Bocchi, S., 2009. Plant nitrogen concentration in
817 paddy rice from field canopy hyperspectral radiometry. F. Crop. Res. 111, 119–129.

818 Thompson, R.L., Lassaletta, L., Patra, P.K., Wilson, C., Wells, K.C., Gressent, A., Koffi, E.N.,
819 Chipperfield, M.P., Winiwarter, W., Davidson, E.A., 2019. Acceleration of global N 2 O
820 emissions seen from two decades of atmospheric inversion. Nat. Clim. Chang. 9, 993–998.

821 Tian, Y.C., Yao, X., Yang, J., Cao, W.X., Hannaway, D.B., Zhu, Y., 2011. Assessing newly
822 developed and published vegetation indices for estimating rice leaf nitrogen concentration
823 with ground-and space-based hyperspectral reflectance. F. Crop. Res. 120, 299–310.

824 Tilling, A.K., O'Leary, G.J., Ferwerda, J.G., Jones, S.D., Fitzgerald, G.J., Rodriguez, D.,
825 Belford, R., 2007. Remote sensing of nitrogen and water stress in wheat. F. Crop. Res.
826 104, 77–85.

827 Trotter, G.M., Whitehead, D., Pinkney, E.J., 2002. The photochemical reflectance index as a
828 measure of photosynthetic light use efficiency for plants with varying foliar nitrogen
829 contents. Int. J. Remote Sens. 23, 1207–1212.

830 Van Leeuwen, W.J.D., Huete, A.R., 1996. Effects of standing litter on the biophysical
831 interpretation of plant canopies with spectral indices. Remote Sens. Environ. 55, 123–138.

832 Varco, J.J., Fox, A.A., Raper, T.B., Hubbard, K.J., 2013. Development of sensor based
833 detection of crop nitrogen status for utilization in variable rate nitrogen fertilization, in:
834 Precision Agriculture'13. Springer, pp. 145–150.

835 Viña, A., Gitelson, A.A., Nguy-Robertson, A.L., Peng, Y., 2011. Comparison of different
836 vegetation indices for the remote assessment of green leaf area index of crops. Remote
837 Sens. Environ. 115, 3468–3478.

838 Wang, Z.-H., Li, S.-X., 2019. Nitrate N loss by leaching and surface runoff in agricultural land:
839 A global issue (a review), in: Advances in Agronomy. Elsevier, pp. 159–217.

840 Xu, X., Zhao, C., Wang, J., Zhang, J., Song, X., 2014. Using optimal combination method and
841 in situ hyperspectral measurements to estimate leaf nitrogen concentration in barley.
842 Precis. Agric. 15, 227–240.

843 Yao, X., Ren, H., Cao, Z., Tian, Y., Cao, W., Zhu, Y., Cheng, T., 2014. Detecting leaf nitrogen

content in wheat with canopy hyperspectrum under different soil backgrounds. Int. J. Appl. Earth Obs. Geoinf. 32, 114–124.

Yoder, B.J., Pettigrew-Crosby, R.E., 1995. Predicting nitrogen and chlorophyll content and concentrations from reflectance spectra (400–2500 nm) at leaf and canopy scales. Remote Sens. Environ. 53, 199–211.

Zarate-Valdez, J.L., Whiting, M.L., Lampinen, B.D., Metcalf, S., Ustin, S.L., Brown, P.H., 2012. Prediction of leaf area index in almonds by vegetation indexes. Comput. Electron. Agric. 85, 24–32.

Zhai, Y., Zhao, X., Teng, Y., Li, X., Zhang, J., Wu, J., Zuo, R., 2017. Groundwater nitrate pollution and human health risk assessment by using HHRA model in an agricultural area, NE China. Ecotoxicol. Environ. Saf. 137, 130–142.

Zhang, J.-H., Ke, W., Bailey, J.S., Ren-Chao, W., 2006. Predicting nitrogen status of rice using multispectral data at canopy scale. Pedosphere 16, 108–117.